Stability and mechanical properties of various Hf–H phases: A density-functional theory study*

Wei Xiao(肖伟)[1,2], Lu Sun(孙璐)[1], Shu-Hui Huang(黄树晖)[1], Jian-Wei Wang(王建伟)[1], Lei Cheng(程磊)[1], and Li-Gen Wang(王立根)[1,†]

[1] *General Research Institute for Nonferrous Metals, Beijing* 100088, *China*

[2] *University of Science and Technology Beijing, Beijing* 100083, *China*

(Received 10 May 2017; revised manuscript received 10 July 2017; published online 10 September 2017)

We performe first-principles density functional theory calculations to investigate the stability and mechanical properties of various HfH_x ($0 \leq x \leq 1$) phases. For pure Hf phases, the calculated results show that the HCP and FCC phases are mechanically stable, while the BCC phase is unstable at 0 K. Also, as for various HfH_x phases, we find that H location and concentration could have a significant effect on their stability and mechanical properties. When $0 \leq x \leq 0.25$, the HCP phases with H at (tetrahedral) T sites are energetically most stable among various phases. The FCC and BCC phases with H at T sites turn to be relatively more favorable than the HCP phase when H concentration is higher than 0.25. Furthermore, our calculated results indicate that the H solution in Hf can largely affect their mechanical properties such as the bulk moduli (B) and shear moduli (G).

Keywords: first-principles, hafnium, hydrogen

PACS: 61.82.Bg, 62.20.–x, 71.15.Mb, 71.15.NC **DOI:** 10.1088/1674-1056/26/10/106103

1. Introduction

Hafnium (Hf), a typical group IVB metal, has wide applications in nuclear technology and modern manufacture.[1,2] Due to its properties of adequate plasticity, easy processing, and high-temperature corrosion resistance, Hf has been always used as the neutron absorbers for control rods in nuclear reactors. It is also the principal gate or electrode material in metal–oxide semiconductor field effect transistors (MOSFETs) in the field of modern semiconductors. In addition, it can be added into tungsten, molybdenum, tantalum, tantalum, and other alloys for property improvement.

Chemically similar to Zr, Hf can easily hydride. By means of differential scanning calorimetry (DSC), Ogiyanagi *et al.* have measured terminal solid solubility of hydrogen for nonirradiated Hf, and found that the hydrogen concentration was in the range of [27, 300] wt ppm.[3] Using nuclear magnetic resonance (NMR), Gotteald *et al.* have studied the hydrogen diffusion in Hf, and obtained that the activation enthalpy for hydrogen diffusion increases slightly with hydrogen concentration.[4] Also, nowadays many experiments have already testified that the structure, phase transformations, and physical properties of Hf–H phases differ largely from the pure ones. Sidhu and Mcguire have obtained three phases of the Hf–H system at room temperature, i.e., deformed cubic phase, face-centered cubic (FCC) phase, and face-centered tetragonal (FCT) phase.[5] Using the time-dependent perturbed angular correlation (TDPAC) technique, Berant *et al.* have demonstrated that when the H/Hf atom ratio is less than 1.63, Hf–H systems are mainly composed of metallic hexagonal-close-packed (HCP) Hf and hydride FCC phases.[6] However, the related theoretical studies for the Hf–H system are inadequate. Thus, a systematic research of various types of Hf and Hf–H phases could help exploring potential applications of this important metal.

In this paper, we will carry out a systematic study on the stability and mechanical properties of various Hf and Hf–H phases by performing first-principles calculations. Three structures of HCP, FCC, and BCC are taken into accounts in the study. For each Hf structure, H atom has been placed at tetrahedral (T) and octahedral (O) interstitial sites, respectively. Here, H concentration is only restricted in the low concentration range of $0 \leq x \leq 1$. Our studies mainly focus on the effects of H location and concentration on the properties of various Hf–H phases, which can help us gain a deep insight into the Hf–H interactions.

We will organize the remainder of the paper as follows. In Section 2, the theoretical methods and the computational details are described. Section 3 presents our calculated results of structural stability and mechanical properties of Hf and Hf–H phases. The effects of H location and concentration on the stability and mechanical properties of Hf–H phases have also been discussed in detail in this section. Finally, a short sum-

*Project supported by the National Natural Science Foundation of China (Grant Nos. 51401030 and 51504033).

†Corresponding author. E-mail: lg_wang1@yahoo.com

© 2017 Chinese Physical Society and IOP Publishing Ltd

mary is given in the last section.

2. Computational details

The first-principles calculations in the framework of density functional theory (DFT) are performed using Vienna *Ab-initio* Simulation Package (VASP).[7,8] The electron–ion interaction is described using projector augmented wave method,[9,10] the exchange–correlation between electrons using generalized gradient approximation (GGA) in the Perdew–Burke–Ernzerhof (PBE) form.[11] The energy cutoff for the plane wave basis set is 300 eV for all calculations. In this study, we will change H concentration by using different sizes of supercells. Seven different kinds of H concentrations have been employed, i.e., $Hf_{32}H$, $Hf_{16}H$, Hf_8H, Hf_4H, Hf_2H, Hf_2H_2, and pure Hf phases. These supercell models contain 32, 16, 8, 4, 2, 2, and 2 Hf atoms, respectively. For these three types of crystal lattices, we all have taken test calculations for k-point convergence. As a result, for pure Hf, Hf_2H_2, Hf_2H, Hf_4H, Hf_8H, $Hf_{16}H$, and $Hf_{32}H$ phases with BCC structures, the k-meshes of $14\times14\times14$, $14\times14\times14$, $14\times14\times14$, $10\times10\times10$, $10\times10\times10$, $8\times8\times8$, and $6\times6\times6$ are adopted for geometry optimization, respectively. For the supercells with FCC structures, we used the k-meshes of $17\times17\times17$, $17\times17\times17$, $17\times17\times17$, $12\times12\times12$, $10\times10\times10$, $9\times9\times6$, and $6\times6\times6$, respectively, while the k-meshes are $15\times15\times10$, $15\times15\times10$, $15\times15\times10$, $15\times10\times10$, $8\times10\times10$, $8\times8\times5$, and $8\times5\times5$ for the systems of HCP structures, respectively. The supercell parameters and the atomic positions are allowed to relax until the forces on all atoms are converged to 0.05 eV/Å.

3. Results and discussions

3.1. Stability and mechanics of pure Hf phases

For the sake of comparison, at first we calculate lattice constants of the HCP, FCC, and BCC phases for pure Hf. The corresponding values are listed in Table 1. For pure Hf phases, we obtain the lattice constants of $a = 3.20$ Å and $c = 5.04$ Å for the HCP structure, $a = 4.47$ Å for the FCC structure, and $a = 3.53$ Å for the BCC structure, which match well with the previous experiments[12–15] and calculations.[16] This further confirms that the computation parameters are properly chosen.

The independent elastic constants for pure HCP, FCC, and BCC Hf phases can be directly obtained from the VASP calculations. The corresponding results for pure HCP, FCC, and BCC Hf phases are also listed in Table 1. For example, the elastic constants C_{11}, C_{12}, C_{13}, C_{33}, and C_{44} of the HCP Hf phase we obtain are 200, 64, 73, 201, and 54 GPa, respectively. These data are consistent with Fisher and Renken's experimental results,[13,14] which again verifies the accuracy of our DFT calculations. Based on these data we can predict their mechanical properties theoretically. The bulk moduli (B) and Young's moduli (E) of crystalline Hf phases are calculated by fitting the Murnaghan equation of state (EOS) and Voigt–Reuss–Hill approximation,[17] respectively. Then, we can obtain E of crystalline Hf phases through the following equation

$$E = \frac{9BG}{3B+G}. \tag{1}$$

Table 1. The calculated results of lattice constants (in unit Å), elastic constants (GPa), and mechanical properties (GPa) of pure Hf phases. The corresponding results in previous experiments[12–15] and calculations[16] are also given in parenthesis for comparison.

Hf phases	a/Å	c/Å	C_{11}/GPa	C_{12}/GPa	C_{13}/GPa	C_{33}/GPa	C_{44}/GPa	B/GPa	G/GPa	E/GPa
HCP[12–14]	3.20 (3.19)	5.04 (5.05)	200 (188)	64 (77)	73 (66)	201 (197)	54 (56)	109 (110)	60 (30)	151 (78)
FCC[16]	4.47 (4.44)	–	145	89	89	145	65	108	50	130
BCC[15]	3.53 (3.62)	–	78	119	119	78	51	105	22	62

As listed in Table 1, we can see that the theoretical value of B agrees well with experiments while E dose not. It attributes to that the Voigt–Reuss–Hill approximation could produce a big error by the large anisotropy of the structures.[17] Due to the overestimation of G, the predicted E also deviates from the experimental values.

With reference to HCP Hf phases, we obtain the structural energy difference is 0.18 eV/atom and 0.07 eV/atom for BCC and FCC Hf phases, respectively. Therefore, we correctly predict that the HCP phase is the ground state for Hf metal. Also, according to the strain energy theory, the independent elastic constants of a mechanically stable phase should satisfy several restrictions. For a cubic crystal, the stability criteria are $C_{11} > 0$, $C_{11}^2 > C_{12}^2$, and $C_{44} > 0$, while for an HCP crystal they are $C_{11} > 0$, $C_{11}^2 > C_{12}^2$, $C_{33}(C_{11}+C_{12}) > C_{13}^2$, and $C_{11}C_{33} > C_{13}^2$. Thus, from Table 1, we can see the HCP and FCC structures satisfy the stability criteria, which implies that these phases could be mechanically stable. However, as for the BCC structure, the value of C_{12} is larger than its C_{11} by 41 GPa, which means it is mechanically unstable at 0 K. These results are consistent with the Hf–H phase diagram[18] that shows BCC Hf phases only exist at high temperatures. Xie *et al.* have discussed why the HCP and BCC phases can exist naturally, but not for the FCC phase.[19] Interestingly, the

mechanically stable FCC phase cannot exist naturally, while unstable BCC can exist.

3.2. Stability and mechanical properties of Hf–H phases

The effects of H on structural stability and mechanical properties of various Hf–H phases are very significant. Here, we have modeled seven different kinds of H concentration of HfH_x phases. The calculated atomic volumes of various HfH_x phases as a function of H/Hf atom ratio are depicted in Fig. 1. It shows that all the HfH_x phases experience volume expansion with the addition of H, and the atomic volumes of HfH_x phases almost increase linearly with H concentration. As clearly shown in Fig. 1, we can see for the pure phases, the BCC Hf phase has the smallest volume of 22.01 $Å^3$. When $0 < x < 0.125$, the differences of these six phases are relatively negligible. However, when $0.125 < x \leq 1$, the distinction of the six curves in Fig. 1 is apparent. The six curves can be divided into two parts and the volume expansion of T sites are distinctly larger than the corresponding O sites. These results suggest that H location and concentration in Hf should have a strong impact on volume expansion especially when the H concentration increases beyond 0.125.

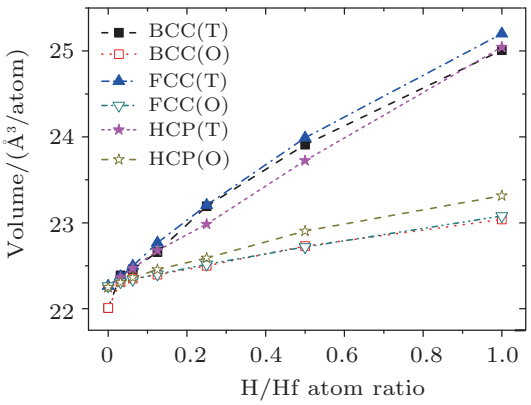


Fig. 1. (color online) Atomic volumes of HfH_x phases as a function of hydrogen concentration.

To evaluate the effect of H on the structural stability of HfH_x phases, we have calculated the formation heat $\triangle H_f$ by the following formula:

$$\triangle H_f = \frac{E_{Hf_nH} - nE_{Hf} - (1/2)E_{H_2}}{n+1}, \quad (2)$$

where E_{Hf_nH}, E_{Hf}, and E_{H_2} are total free energies of Hf_nH, pure HCP Hf, and H_2 molecules, respectively. The calculated results of the formation heat of HfH_x phases as a function of hydrogen concentration are shown in Fig. 2. At first glance, we can see that the formation heat almost decreases linearly with the increase of H concentration x. This phenomenon is also observed for Zr alloys.[20] The slopes of the $\triangle H_f$ for BCC(T), BCC(O), FCC(T), FCC(O), HCP(T), and HCP(O) are calculated through a linear fitting to be −37, −29, −37, −30, −20, and −19 kJ/mol·H respectively, which match well with the experimental value of −38 kJ/mol·H.[21] These calculated values are less than that of Zr alloys (−50 kJ/mol·H) just as the experiment observes. Also, we can find when $0 \leq x \leq 0.25$, HCP(T) phases are energetically more stable than other phases. When H concentration increases to 0.5, FCC(T) and BCC(T) phases turn to be relatively more favorable, and FCC(T) phases have the lowest value of $\triangle H_f$ when $0.5 \leq x \leq 1$. As in Berant *et al.*'s work, it indicated that the HfH_x systems consist chiefly of FCC phases rather than HCP phases when the H/Hf atom ratio reaches 1.63,[6] we can expect the phase transition occurs in this relatively high H concentration.

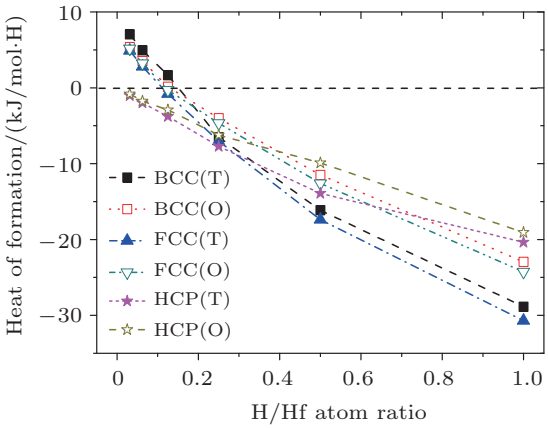


Fig. 2. (color online) Heats of formation of HfH_x phases as a function of hydrogen concentration.

We can see within the entire H concentration only the HCP phases have always a negative ΔH_f and HCP(T) phases are more negative ones. This means H atoms are energetically more favorable to occupy the T sites in HCP Hf phases. For BCC and FCC structures, ΔH_f is not negative until the H/Hf atom ratio surpasses 0.125 and 0.0625, respectively. Just like HCP structures, FCC(T) phases are always energetically favorable ones when compared to FCC(O) phases. As to BCC phases, H prefers O sites when $0 < x < 0.25$ and T sites at the range of $0.25 \leq x \leq 1$. These results demonstrate that the value of ΔH_f depends to a large extent on H concentration, which will play an important role in relative structural stability for these HfH_x phases. For the mechanical properties, we find H addition into Hf can also cause some dramatic changes. Here, by comparing stable HCP(T) Hf_2H phases with pure HCP Hf phases, it is found that H at T sites can increase B by 27% and decrease G by 36%. This trend has been well discussed in Zr–H phases by Wang and Gong.[20] The theoretical computation predicts that the structural stability and mechanical properties have been significantly affected when H is added in Hf, which is consistent with the experiments.[5,6]

In order to elucidate the underlying mechanisms, now we analyze the Hf–H bond length and the densities of states for

the HfH_x phases. Taking the stable HCP phases as an example, we present the average bond length $\overline{d}_{Hf-H}$ of HCP(T) and HCP(O) HfH_x phases as a function of hydrogen concentration in Fig. 3. It shows that the values of $\overline{d}_{Hf-H}$ almost keep the same although the H concentration changes. In addition, from Fig. 3 we can check that the $\overline{d}_{Hf-H}$ in HCP(T) phases is about [1.99, 2.03] Å while the HCP(O) phases have a larger $\overline{d}_{Hf-H}$ of about [2.27, 2.30] Å. When H is located in the T and O sites of FCC or BCC phases, the bond lengths between Hf and H are still in the same range. So it can be expected that the degree of the volume expansion is mainly determined by the the number of H atoms. These can well explain why the atomic volumes of HfH_x phases almost increases linearly with the H concentration.

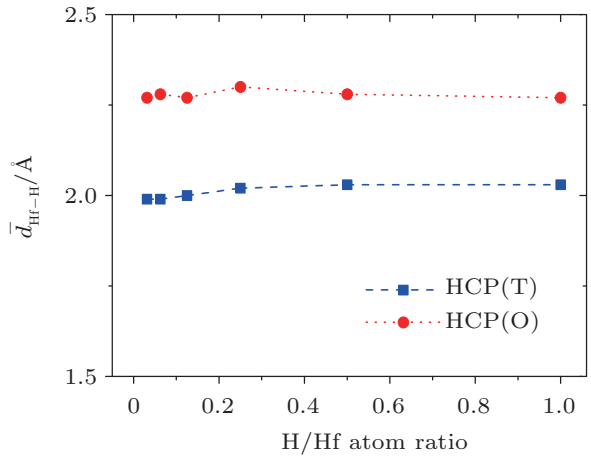


Fig. 3. (color online) The average bond length $\overline{d}_{Hf-H}$ (Å) of HCP(T) and HCP(O) HfH_x phases as a function of hydrogen concentration.

On the other side, to illustrate the change of the electronic properties caused by H solution, we plot in Fig. 4 the calculated density of states (DOS) of the HCP Hf_2 phase and Hf_2H phases with H at both T and O sites for comparison. As clearly shown in Figs. 4(b) and 4(c), we can see that there appears an energy overlap of the Hf-d and H-s states at the energy region of $[-9, -6]$ eV, which means that these two orbitals hybrid strongly with each other. Through the Bader charge analysis, the electron transfers for the two systems are calculated. It is found that in the HCP(T) Hf_2H phase, H totally gains 0.79 electrons from Hf atoms while the number is less by 0.12 electrons in the HCP(O) Hf_2H phase, suggesting that the chemical bonding between H and Hf should be stronger when H resides at T sites than at O sites of HCP Hf phases. These are mainly caused by the shorter average bond length between H and Hf atoms. Also, figure 4 displays that the Fermi level of the pure HCP Hf phases is situated at the bottom of the peseudogap, while the Fermi level of HCP(T) and HCP(O) Hf_2H phases moves towards the DOS peak. The DOS at the Fermi level is 0.85 states/eV·atom and 1.17 states/eV·atom for HCP(T) and HCP(O) Hf_2H phases, respectively. The larger value means more brittle. Thus, the structural and physical properties of Hf can be largely affected by H atoms.

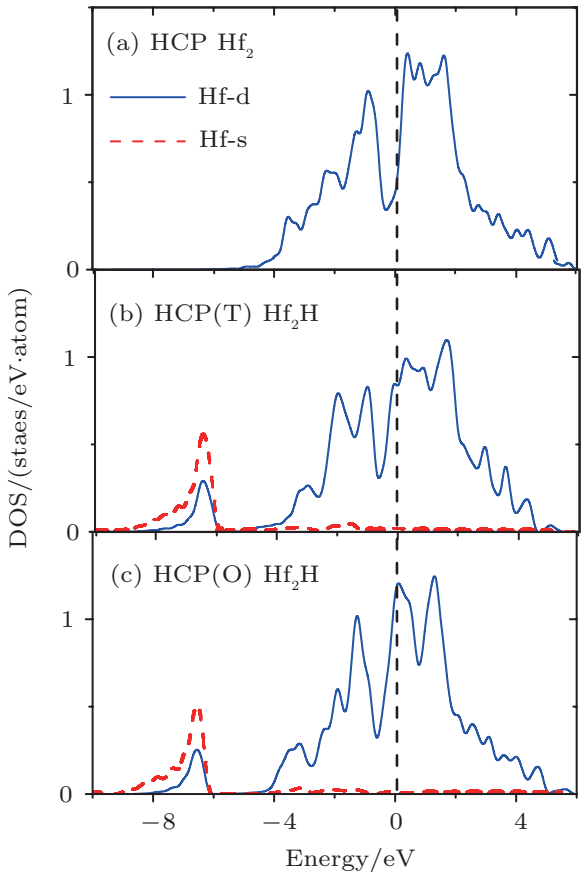


Fig. 4. (color online) Comparison of densities of states of (a) the HCP Hf_2 phase and (b) HCP(T), and (c) HCP(O) Hf_2H phases. The red and blue curves represent H-s and Hf-d DOS, respectively. The Fermi energy is shifted to 0 eV.

4. Conclusions

By employing first-principles density functional theory calculations, we have investigated the stability and mechanical properties of Hf and HfH_x ($0 \leq x \leq 1$) phases. For pure Hf phases, the structural and mechanical properties for three types of phases (HCP, FCC, and BCC) have been presented. The calculated results have showed that the HCP phase is the ground state and the BCC phase is mechanically unstable at 0 K. Also, our calculations for HfH_x ($0 \leq x \leq 1$) phases have demonstrated that H location and concentration could have a significant effect on the stability of the corresponding Hf–H phases. When $0 \leq x \leq 0.25$, the HCP phases with H at T sites are energetically more stable among these structures, while H concentration increases to 0.5, the FCC and BCC phases with H at T sites turn to be relatively more favorable. In addition, by comparing HCP(T) Hf_2H phases with pure HCP Hf, it is found that H addition could affect the mechanical properties by decreasing bulk moduli and increasing shear moduli. On the whole, the stability and mechanical properties of various HfH_x ($0 \leq x \leq 1$) phases obtained in our calculations are in

good agreement with the experimental data available in the literature. These results can be deeply understood by the electronic structure and bond length analysis.

References

[1] Habashi F 2013 *Hafnium, Physical and Chemical Properties* (New York: Springer)
[2] Risovanyi V D, Klochkov E P and Varlashova E E 1996 *At. Energy* **81** 764
[3] Ogiyanagi J, Chimi Y, Shimada S, Nakamura T and Abe K 2010 *J. Nucl. Sci. Technol.* **47** 197
[4] Gottwald J, Majerb G, Petersonc D T and Barnesc R G 2003 *J. Alloys Compd.* **356–357** 274
[5] Sidhu S S and Mcguire J C 1952 *J. Appl. Phys.* **23** 1257
[6] Berant Z, *et al*. 1989 *Hyperfine Interact.* **52** 383
[7] Kresse G and Furthmuller J 1996 *Comput. Mater. Sci.* **6** 15
[8] Kresse G and Furthmuller J 1996 *Phys. Rev. B* **54** 11169
[9] Blochl P E 1994 *Phys. Rev. B* **50** 17953
[10] Kresse G and Joubert D 1999 *Phys. Rev. B* **59** 1758
[11] Perdew J P, Burke K and Ernzerhof M 1996 *Phys. Rev. Lett.* **77** 3865
[12] Glaser F W, Moskowitz D and Post B 1953 *J. Met.* **5** 1119
[13] https://en.wikipedia.org/wiki/Hafnium
[14] Fisher E S and Renken C J 1964 *Phys. Rev.* **135** A482
[15] Romans P A, Paasche O G and Kato H 1965 *J. Alloys Compd.* **8** 213
[16] Häglund J, Fernádez Guillermet A, Grimvall G and Körling M 1993 *Phys. Rev. B* **48** 11685
[17] Westbrook J H and Fleischer R L 1995 *Intermetallic compounds: principles practice, volume I: principles* (John Wiley Sons)
[18] Predel B 1996 *H–Hf (Hydrogen–Hafnium), Ga–Gd — Hf–Zr* (Berlin, Heidelberg: Springer)
[19] Xie Y Q, Peng K and Yang X X 2001 *J. Cent. South Univ. Thchnol.* **8** 83
[20] Wang F and Gong H R 2012 *Int. J. Hydrogen Energy* **37** 12393
[21] Schlapbach L 1988 *Hydrogen in intermetallic compounds I* (Berlin, Heidelberg: Springer)